Special Issue Article

Advances in Mechanical Engineering

Advances in Mechanical Engineering
2016, Vol. 8(4) 1–12

DOI: 10.1177/1687814016642670
aime.sagepub.com
SAGE

Improved nonlinear sliding mode control based on load disturbance observer for permanent magnet synchronous motor servo system

Rongrong Qian[1], Minzhou Luo[2] and Peng Sun[2]

Abstract

This article presented an improved nonlinear sliding mode control based on disturbance observer for the permanent magnet synchronous motor servo system. The position transient response performances, such as fast response and non-overshoot, are enhanced by the introduction of novel nonlinear sliding surface in the design of sliding mode control law. In order to abolish the analysis necessity of changeable uncertainties and alleviate the system chattering, the nonlinear sliding mode control algorithm is improved by adaptive parameter estimation and saturation function. Since the improved nonlinear sliding mode control algorithm is sensitive to mismatched uncertainties which are mainly due to the load disturbance, a disturbance observer is put forward to estimate the mismatched uncertainties and is integrated into control law design to improve the positioning accuracy. The stability of improved nonlinear sliding mode control based on disturbance observer is proved based on the Lyapunov approach. The simulation results demonstrate the effectiveness and robustness of the proposed improved nonlinear sliding mode control based on disturbance observer for permanent magnet synchronous motor servo system with stationary and dynamic trajectory tracking.

Keywords

Nonlinear sliding mode control, mismatched uncertainties, disturbance observer, adaptive parameter estimation, permanent magnet synchronous motor servo system

Date received: 24 September 2015; accepted: 9 March 2016

Academic Editor: Nasim Ullah

Introduction

The permanent magnet synchronous motor (PMSM) has been widely used in many fields, such as high-performance computer numerical control (CNC) system, aerospace industry, and robot, owing to its advantages including compact structure, high power density, high inertia torque ratio, and high efficiency.[1] In order to acquire fast four-quadrant operation and smooth start and acceleration, the field-oriented control or space vector control is employed in the design of PMSM drive.[2–4] However, PMSM is a time-varying nonlinear system with multivariable and strong coupling and easily influenced by the external interference. Furthermore, the model parameter mismatch and perturbation existed in the PMSM mathematical model of field-oriented control system since the model is built in the hypothesis of neglecting the influence of magnetic circuit saturation, hysteresis, and eddy current. Therefore, the traditional proportional–integral (PI)

[1]School of Information Science and Technology, University of Science and Technology of China, Hefei, China
[2]Institute of Advanced Manufacturing Technology, Hefei Institutes of Physical Science, Chinese Academy of Sciences, Changzhou, China

Corresponding author:
Peng Sun, Institute of Advanced Manufacturing Technology, Hefei Institutes of Physical Science, Chinese Academy of Sciences, Changzhou 213164, Jiangsu, China.
Email: psun@iamt.cas.cn

controller is unable to satisfy the dynamic response performance of PMSM due to its fixed proportional gain and integral time constant.[5–7] In recent years, many nonlinear control strategies have been developed for PMSM servo system to improve the dynamic response such as neural-based robust control algorithms,[7–9] adaptive control,[10–13] H_∞ control,[14] and sliding mode control (SMC).[3,4]

The SMC is employed frequently in the AC servo control system due to its good performance of fast response and insensitivity to the matched parameter perturbation and disturbance. The principle for designing SMC is to construct the sliding surface based on the system state variables. Zhang and Panda[15] presented the conventional linear sliding surface (LSS) used in PMSM speed control to make the system convergent within finite settling time. The non-singular terminal sliding mode manifold is proposed in PMSM speed regulation system to obtain a faster convergent speed and a better tracking precision.[16] Recently, SMC has been combined with intelligent control method to achieve better performance of PMSM control.[17,18] However, according to the control law design of traditional SMC system with mismatched uncertainties, the states can only be driven to the sliding surface in finite time rather than the desired equilibrium. This leads to many researches on the SMC design for uncertain systems with mismatched uncertainties. The linear matrix inequality (LMI)-based sliding surface design for SMC has been proposed to guarantee the asymptotic stability of full order system with mismatched uncertainties.[19–21] The disturbance observer (DOB) is also integrated into the SMC to counteract the mismatched disturbance.[19–23] Yet, the transient response performances of the systems are rarely considered in these researches.

Actually, in the control systems, settling time, rising time, and overshoot are the main indexes for transient response. The fast settling and rising time with non-overshoot are necessary for many systems, such as aircraft control system, electromechanical control system, and power converter. However, the settling time and system stability are in conflict with each other, which means small settling time for systems will lead to high overshoot and vice versa. In order to increase the response speed of closed-loop system and reduce the overshoot, a composite nonlinear feedback (CNF) tracking control law is proposed which has a gradually increasing damping ratio with small initial value.[24] The principle is that in the initial state the system has a small damping ratio but fast response and along with the system output getting close to the desired value, the damping ratio is getting bigger to avoid the overshoot. The nonlinear sliding surface on the basis of CNF is presented to improve the convergence performance of system based on SMC algorithm.[25]

However, the research of SMC with nonlinear sliding surface is under two preconditions. One is the prior knowledge of the matched parameter perturbation and external disturbance, and the other is that the mismatched disturbance of system is neglected. Both preconditions are hardly satisfied in most industrial applications. Then consequently, the improved nonlinear sliding mode control based on load disturbance observer (NSMC-DOB) is proposed in this article. In order to verify the feasibility of the proposed control law, the PMSM position servo system is used as the controlled plant. This article is organized as follows. First, when the mismatched disturbance is neglected and the prior knowledge of the matched disturbance is hypothesized as known, the nonlinear sliding mode control (NSMC) is used for PMSM servo system. This system has the distinct advantage of good transient response performance with fast response and non-overshoot. The prior knowledge of matched parameter perturbation and disturbance is used for determining the switching gain in SMC and is hard to determine. Therefore, the adaptive parameter estimation is designed to establish the switching gain. Meanwhile, the saturation function is combined to design the improved NSMC to reduce the system chattering under the condition of permissible system errors. In the PMSM servo system, the mismatched uncertainty is mainly due to the load disturbance. A DOB is designed to deal with the problem that the improved NSMC is sensitive to mismatched uncertainty. The new sliding surface is designed by combining the nonlinear sliding surface with DOB. The corresponding control law of realizing the robustness to the mismatched perturbations is also acquired and the stability analysis is deduced. At last, the effectiveness and robustness of the proposed improved NSMC-DOB for PMSM servo system are demonstrated by the simulation results with stationary and dynamic trajectory tracking.

Mathematical model of PMSM

The proposed control system is based on the surface-mounted PMSM in which d and q axis stator inductance can be considered as $L_d = L_q = L_s$. Considering that the space magnetic field is distributed as sinusoidal field and neglecting the influence of magnetic circuit saturation, hysteresis, and eddy current, the continuous mathematical model for PMSM in d-q frame is as follows

$$u_d = R_s i_d + L_s \frac{di_d}{dt} - L_s \omega_e i_q \tag{1}$$

$$u_q = R_s i_q + L_s \frac{di_q}{dt} + L_s \omega_e i_d + \omega_e \varphi_m \tag{2}$$

$$T_e = J_m \frac{d\omega_r}{dt} + B_m \omega_r + T_l \tag{3}$$

$$T_e = \frac{3}{2} p \varphi_m i_q \tag{4}$$

$$\omega_e = p \omega_r \tag{5}$$

It can be clearly seen from equations (1) to (3) that PMSM vector control system has a strong coupling between i_d, i_q, and ω_e. In order to decouple and be appropriate for analyzing and designing the NSMC, the auxiliary input variables are defined as

$$v_d = \frac{u_d}{L_s} + \omega_e i_q \tag{6}$$

$$v_q = \frac{u_q}{L_s} - \omega_e i_d \tag{7}$$

Supposed that $\rho(t) = [\rho_{d1}(t),\ \rho_{d2}(t)]^{\mathrm{T}}$ is the continuous and bounded matched disturbance and parameter perturbation related to the system control input u_d, u_q and the boundary is defined as

$$\rho^* = \max(\rho_{d1}^*, \rho_{d2}^*) = \max(\sup_{t>0}(|\rho_{d1}(t), \rho_{d2}(t)|)) \tag{8}$$

Combining lumping uncertainties and load disturbance and using the feedback linearization by substituting above auxiliary input variables (6), (7) to get the linear PMSM *d-q* frame model as follows

$$\begin{bmatrix} \dot{\omega}_e \\ \dot{\theta}_e \\ \dot{i}_d \\ \dot{i}_q \end{bmatrix} = \begin{bmatrix} -\frac{B_m}{J_m} & 0 & 0 & \frac{1.5p^2\varphi_m}{J_m} \\ 1 & 0 & 0 & 0 \\ 0 & 0 & -\frac{R_s}{L_s} & 0 \\ -\frac{\varphi_m}{L_s} & 0 & 0 & -\frac{R_s}{L_s} \end{bmatrix} \begin{bmatrix} \omega_e \\ \theta_e \\ i_d \\ i_q \end{bmatrix} + \begin{bmatrix} 0 & 0 \\ 0 & 0 \\ 1 & 0 \\ 0 & 1 \end{bmatrix} \begin{bmatrix} v_d \\ v_q \end{bmatrix} + \begin{bmatrix} \frac{p}{J_m} \\ 0 \\ 0 \\ 0 \end{bmatrix} T_l + \begin{bmatrix} 0 \\ 0 \\ \rho_{d1}(t) \\ \rho_{d2}(t) \end{bmatrix} \tag{9}$$

Remark. Supposed that parameter perturbations of J_m and B_m are all attributed to the load disturbance T_l which is considered as mismatched uncertainties for the controlled system in this article.

Improved NSMC-DOB for PMSM servo system

NSMC for PMSM servo system without load disturbance

The novel nonlinear sliding surface is put forward for controlled system with matched uncertainties by Bijnan Bandyopadhyay et al.[25] Based on the nonlinear sliding surface, the system transient response performance is improved by the variable system damping ratio. The following system in regular form without load disturbance deduced from equation (9) is generally used to derive the NSMC algorithm

$$\begin{cases} \dot{x}_1(t) = A_{11}x_1(t) + A_{12}x_2(t) \\ \dot{x}_2(t) = A_{21}x_1(t) + A_{22}x_2(t) + u(t) + \rho(t) \end{cases} \tag{10}$$

$$y(t) = Cx(t) \tag{11}$$

where $x(t) = [x_1(t),\ x_2(t)]^{\mathrm{T}}$. $x_1(t) = [\omega_e(t),\ \theta_e(t)]^{\mathrm{T}}$ and $x_2(t) = [i_d(t),\ i_q(t)]^{\mathrm{T}}$ are the mismatched and matched state variables with the control input, respectively

$$u(t) = \begin{bmatrix} u_d \\ u_q \end{bmatrix},\ \rho(t) = \begin{bmatrix} \rho_{d1}(t) \\ \rho_{d2}(t) \end{bmatrix},\ A = \begin{bmatrix} A_{11} & A_{12} \\ A_{21} & A_{22} \end{bmatrix}$$

$$A_{11} = \begin{bmatrix} -\frac{B_m}{J_m} & 0 \\ 1 & 0 \end{bmatrix},\ A_{12} = \begin{bmatrix} 0 & \frac{1.5p^2\varphi_m}{J_m} \\ 0 & 0 \end{bmatrix},$$

$$A_{21} = \begin{bmatrix} 0 & 0 \\ -\frac{\varphi_m}{L_s} & 0 \end{bmatrix}$$

$$A_{22} = \begin{bmatrix} -\frac{R_s}{L_s} & 0 \\ 0 & -\frac{R_s}{L_s} \end{bmatrix},\ C = \begin{bmatrix} 1 & 0 & 0 & 0 \end{bmatrix}$$

The reference trajectory $x_{1\_ref}(t) = [\omega_{e\_ref},\ \theta_{e\_ref}]^{\mathrm{T}}$, $x_{2\_ref}(t) = [i_{d\_ref}(t),\ i_{q\_ref}(t)]^{\mathrm{T}}$ for PMSM servo system can be acquired from the nominal PMSM model (1)–(5) and the variable error can be defined as

$$e_1 = x_{1\_ref} - x_1 \tag{12}$$

$$e_2 = x_{2\_ref} - x_2 \tag{13}$$

The novel nonlinear sliding surface is defined as

$$s(x,t) = \begin{bmatrix} s_1(x,t) \\ s_2(x,t) \end{bmatrix} = \begin{bmatrix} F - \psi(y,r)A_{12}^T P & I_2 \end{bmatrix} \begin{bmatrix} e_1(t) \\ e_2(t) \end{bmatrix} \tag{14}$$

$$\sigma(t) = \begin{bmatrix} F - \psi(y,r)A_{12}^T P & I_2 \end{bmatrix} \tag{15}$$

$$\delta(t) = F - \psi(y,r)A_{12}^T P \tag{16}$$

where I_2 is a two-dimensional identity matrix and r is the desired rotor electrical angle. F is chosen to satisfy the condition that $(A_{11}–A_{12}F)$ has stable eigenvalues

and the dominant poles have a very low damping ratio.[25] P is the positive definite symmetric matrix calculated from Lyapunov equation below

$$(A_{11} - A_{12}F)^T P + P(A_{11} - A_{12}F) = -W \tag{17}$$

where W is a known positive definite matrix.

$\psi(y,r)$ is a non-positive function and continuously differentiable with respect to y. It is used to increase the damping ratio of the controlled system by changing itself from 0 or a tiny value to a negative constant as the rotor angle is gradually approaching the expected electrical value. In this article, $\psi(y,r)$ is defined as

$$\psi(y,r) = -k(e^{-\beta(y-r)^2}) \tag{18}$$

where $k > 0$, $\beta > 0$, and β should be big enough to make $\psi(y,r)$ to be a tiny value initially.

According to the principle of SMC, the following equation is satisfied when the system states reach the sliding surface

$$s(x,t) = 0 \tag{19}$$

Combining equations (9), (10), and (14) gives

$$e_2(t) = -Fe_1(t) + \psi(y,r)A_{12}^T P e_1(t) \tag{20}$$

$$\dot{e}_1(t) = (A_{11} - A_{12}F + A_{12}\psi(y,r)A_{12}^T P)e_1(t) \tag{21}$$

Equation (20) means that $e_1(t) = 0 \Rightarrow e_2(t) = 0$. Therefore, in order to demonstrate the stability of the system states in the sliding surface, the Lyapunov function can be defined as

$$V_1(t) = e_1^T(t) P e_1(t) \tag{22}$$

Supposed that $M = A_{12}^T P e_1$ and evaluating $\dot{V}_1(t)$ as follows

$$\begin{aligned}\dot{V}_1(t) &= \dot{e}_1^T(t)Pe_1(t) + e_1^T(t)P\dot{e}_1(t)\\ &= e_1^T(t)(A_{11} - A_{12}F)^T Pe_1(t)\\ &\quad + e_1^T(t)P(A_{11} - A_{12}F)e_1(t)\\ &\quad + 2e_1^T(t)PA_{12}\psi(y,r)A_{12}^T Pe_1(t)\\ &= -e_1^T(t)We_1(t) + 2\psi(y,r)M^T M < 0\end{aligned}$$

Therefore, the error state $e_1(t)$ is asymptotic convergence as well as $e_2(t)$.

The control aim of traditional SMC is to design the control input such that the system state trajectory is forced to arrive the predefined sliding surface and converge to the expected value along the sliding surface. Since there are time delay and spatial lag caused by switches in PMSM servo system, the vibration is easily created. Therefore, the exponential approaching law is used in the derivation of SMC. The advantage of the exponential approaching law is that it has a fast system response when the system state is far away from the sliding surface and the convergence speed is approaching zero when the system state is gradually closed to sliding surface. This advantage can reduce the chattering caused by the SMC switching term. The exponential approaching law is defined as

$$\dot{s} = -k_1 s - k_2 \mathrm{sgn}(s) \tag{23}$$

where k_1, k_2 are positive constant.

Combined with the exponential approaching law (23) and differentiating (14) and using (10) we can get the NSMC controller as follows

$$\begin{aligned}u(t) = &-\frac{d}{dt}\psi(y,r)A_{12}^T Pe_1(t) + \sigma(t)\dot{x}_d(t) - \sigma(t)Ax(t)\\ &+ k_1 s + k_2 \mathrm{sgn}(s)\end{aligned} \tag{24}$$

where $x_d = [x_{1\_ref}(t)^{\mathrm{T}}, x_{2\_ref}(t)^{\mathrm{T}}]^{\mathrm{T}}$, $k_1 > 0$, $k_2 > \rho^*$.

Improved NSMC through adaptive parameter estimation and saturation function

The parameter perturbation and disturbance in the PMSM servo system is always unknown and it is difficult to accurately capture the upper bound of uncertainties. Normally in the traditional SMC system the switching gain is chosen to be a high value to satisfy the convergence of control system. Nevertheless, the high switching gain k_2 in the control law (24) will lead to the large fluctuations and thus the system performance is significantly degraded especially for the motor control system with periodically pulse width modulation (PWM) generation mechanism. Therefore, the adaptive parameter estimation is designed to substitute the switching gain for the controller (24) as follows

$$\begin{aligned}u(t) = &-\frac{d}{dt}\psi(y,r)A_{12}^T Pe_1(t) + \sigma(t)\dot{x}_d(t)\\ &- \sigma(t)Ax(t) + k_1 s + \hat{K}(t) * \mathrm{sgn}(s)\end{aligned} \tag{25}$$

As the equation (14) shows that the novel nonlinear sliding surface $s(x,t) \in R^2$ and it means that there are two sliding modes in the control system. Therefore, the adaptive parameter estimations are required respectively for each sliding mode. In order to derive the control law suitable for the matrix calculation, $\hat{K}(t)$ is selected as a diagonal matrix as follows

$$\hat{K}(t) = \begin{bmatrix} \hat{K}_1(t) & 0 \\ 0 & \hat{K}_2(t) \end{bmatrix} \tag{26}$$

$$\dot{\hat{K}}_1(t) = \mu_1 |s_1(x,t)| \tag{27}$$

$$\dot{\hat{K}}_2(t) = \mu_2 |s_2(x,t)| \tag{28}$$

where μ_1, $\mu_2 > 0$ and $\mu_{\min} = \min(\mu_1, \mu_2)$.

Given the system (10) with the controller as (25), the gain $\hat{K}(t)$ has an upper bound, that is, there exists the positive constant matrix $K^* = \begin{bmatrix} K_1^* & 0 \\ 0 & K_2^* \end{bmatrix}$ and it satisfies the condition as follows[26]

$$\forall t > 0, \hat{K}_1(t) < K_1^*, \hat{K}_2(t) < K_2^* \tag{29}$$

According to the SMC stability principle, $\hat{K}(t)$ should satisfy with the condition as follows

$$\forall t > 0,\ \hat{K}_1(t) > \rho_{d1}(t),\ \hat{K}_2(t) > \rho_{d2}(t) \tag{30}$$

The adaptive parameter estimation stability is verified by choosing the Lyapunov function as

$$\begin{aligned} V_2(t) &= \frac{1}{2}s^T s + \frac{1}{2}\gamma(\hat{K}(t) - K^*)^2 \\ &= \frac{1}{2}s^T s + \frac{1}{2}\gamma(\hat{K}_1(t) - K_1^*)^2 + \frac{1}{2}\gamma(\hat{K}_2(t) - K_2^*)^2 \\ &= \frac{1}{2}s_1^2(x,t) + \frac{1}{2}s_2^2(x,t) + \frac{1}{2}\gamma(\hat{K}_1(t) - K_1^*)^2 \\ &\quad + \frac{1}{2}\gamma(\hat{K}_2(t) - K_2^*)^2 \end{aligned} \tag{31}$$

where γ meets the criteria $\gamma\,\mu_{\min} > 1$.

Taking the derivation of the Lyapunov function (31) with control law (25) and (29) yields

$$\begin{aligned} \dot{V}_2(t) &= s^T\dot{s} + \gamma(\hat{K}_1(t) - K_1^*)\dot{\hat{K}}_1(t) + \gamma(\hat{K}_2(t) - K_2^*)\dot{\hat{K}}_2(t) \\ &= s^T(-k_1 s - \hat{K}(t)\mathrm{sgn}(s) + \rho(t)) + \gamma(\hat{K}_1(t) - K_1^*)\dot{\hat{K}}_1(t) \\ &\quad + \gamma(\hat{K}_2(t) - K_2^*)\dot{\hat{K}}_2(t) \\ &< -k_1 s^T s - (K_1^* - |\rho_{d1}(t)|)|s_1(x,t)| \\ &\quad - (K_2^* - |\rho_{d2}(t)|)|s_2(x,t)| \\ &\quad - (K_1^* - \hat{K}_1(t))(\gamma\mu_1|s_1(x,t)| - |s_1(x,t)|) \\ &\quad - (K_2^* - \hat{K}_2(t))(\gamma\mu_2|s_2(x,t)| - |s_2(x,t)|) \\ &= -k_1 s^T s - \beta_1\sqrt{2}\left|\frac{|s_1(x,t)|}{\sqrt{2}}\right| \\ &\quad - \beta_2\sqrt{\frac{2}{\gamma}}\sqrt{\frac{\gamma}{2}}|K_1^* - \hat{K}_1(t)| \\ &\quad - \beta_3\sqrt{2}\left|\frac{|s_2(x,t)|}{\sqrt{2}}\right| - \beta_4\sqrt{\frac{2}{\gamma}}\sqrt{\frac{\gamma}{2}}|K_2^* - \hat{K}_2(t)| \end{aligned}$$

where

$$\beta_1 = K_1^* - |\rho_{d1}(t)| > 0,\ \beta_2 = \gamma\mu_1|s_1(x,t)| - |s_1(x,t)| > 0$$
$$\beta_3 = K_2^* - |\rho_{d2}(t)| > 0,\ \beta_4 = \gamma\mu_2|s_2(x,t)| - |s_2(x,t)| > 0$$

Let $\beta_x = \min\{\beta_1\sqrt{2}, \beta_2\sqrt{2/\gamma}, \beta_3\sqrt{2}, \beta_4\sqrt{2/\gamma}\} > 0$, and based on the following inequality

$$\begin{aligned} V_2^{1/2}(t) &= \left(\frac{1}{2}s_1^2(x,t) + \frac{1}{2}s_2^2(x,t) + \frac{1}{2}\gamma(\hat{K}_1(t) - K_1^*)\right)^2 \\ &\quad + \frac{1}{2}\gamma(\hat{K}_2(t) - K_2^*)^2)^{1/2} \\ &\le \left|\frac{s_1(x,t)}{\sqrt{2}}\right| + \left|\frac{s_2(x,t)}{\sqrt{2}}\right| \\ &\quad + |K_1^* - \hat{K}_1(t)|\sqrt{\frac{\gamma}{2}} + |K_2^* - \hat{K}_2(t)|\sqrt{\frac{\gamma}{2}} \end{aligned}$$

The $\dot{V}_2(t)$ satisfies as

$$\begin{aligned} \dot{V}_2(t) &< -k_1 s^T s \\ &\quad - \beta_x\left(\left|\frac{s_1(x,t)}{\sqrt{2}}\right| + (K_1^* - \hat{K}_1(t))\sqrt{\frac{\gamma}{2}} + \left|\frac{s_2(x,t)}{\sqrt{2}}\right| + (K_2^* - \hat{K}_2(t))\sqrt{\frac{\gamma}{2}}\right) \\ &\le -k_1 s^T s - \beta_x V_2(t)^{1/2} \\ &< 0 \end{aligned} \tag{32}$$

Therefore, the control law (25) can make the system state errors reaching the sliding surface and converge to zero.

Since $|s_i(x,t)|$, $i = 1, 2$ cannot be the absolute zero during the control process, the adaptive parameter estimation will increase infinitely. Therefore, a small value ε is set to modify the adaptive parameter estimation as follows

$$\dot{\hat{K}}(t) = \begin{cases} \mu\begin{bmatrix} |s_1(x,t)| & 0 \\ 0 & |s_2(x,t)| \end{bmatrix}, & \min(|s_1|, |s_2|) \ge \varepsilon \\ 0, & \text{else} \end{cases} \tag{33}$$

where $\mu = \begin{bmatrix} \mu_1 & 0 \\ 0 & \mu_2 \end{bmatrix}$.

A saturation function as equation (34) with a certain threshold value is also used here to instead of sign function to weaken the chattering of the improved NSMC system

$$\mathrm{sat}(u) = \begin{cases} \mathrm{sgn}(u), & |u| > \ell \\ \frac{1}{\ell}u, & |u| \le \ell \end{cases} \tag{34}$$

When $|s_i(x,t)| \ge \ell$, $i = 1,2$, the stability analysis of the sliding modes can be acquired as (33) for the system (10) under the control law (25) with saturation function (34). When $|s_i(x,t)| \le \ell$, $i = 1,2$, the equivalent control diagram of the system is shown in Figure 1, where $u_{eq}(t) = -\frac{d}{dt}\psi(y,r)A_{12}^T P e_1(t) + \sigma(t)\dot{x}_d(t) - \sigma(t)Ax(t)$.

Combining (14) and (25), the following equation is acquired

$$\dot{s}_i(x,t) = -k_1 s_i(x,t) - \frac{\hat{K}_i(t)s_i(x,t)}{\ell} + \rho_{di}(t), \quad i = 1,2 \tag{35}$$

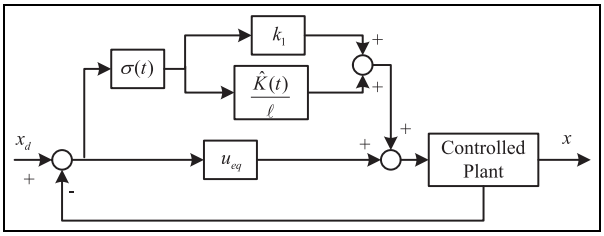

Figure 1. Equivalent control diagram of the system when $|s_i(x,t)| \leqslant \ell$, $i = 1,2$.

The transfer function between $s_i(s)$ and $\rho_{di}(s)$, $i = 1, 2$ can be deduced from (35) as follows

$$s_i(s) = \frac{\rho_{di}(s)}{s + k_1 + \frac{\hat{K}_i(t)}{\ell}}, \quad i = 1, 2 \tag{36}$$

According to the final value theorem, it yields

$$\begin{aligned} \lim_{t\to\infty} s_i(t) &= \lim_{s\to 0} s s_i(s) = \lim_{s\to 0} \frac{s\rho_{di}(s)}{s + k_1 + \frac{\hat{K}_i(t)}{\ell}} \\ &= \frac{1}{k_1 + \frac{\hat{K}_i(t)}{\ell}} \lim_{t\to\infty} \rho_{di}(t) \leq \frac{\rho^*_{di}}{k_1 + \frac{\hat{K}_i(t)}{\ell}}, \quad i = 1, 2 \end{aligned} \tag{37}$$

Since $\psi(y, r)$ is convergent to a constant value as the system output is gradually approaching the expected value, $\sigma(t)$ is also convergent to a constant matrix and it is defined as σ_d. From (14) and (37), the steady error e_{ss} of system states can be deduced as

$$\begin{aligned} e_{ss} &= \lim_{t\to\infty} e(t) = \lim_{t\to\infty} (\sigma^{\mathrm{T}}\sigma)^{-1}\sigma^{\mathrm{T}} s(t) \\ &= (\sigma_d^T\sigma_d)^{-1}\sigma_d^T \lim_{t\to\infty} s(t) \\ &\leq (\sigma_d^T\sigma_d)^{-1}\sigma_d^T \begin{bmatrix} \frac{\rho^*_{d1}}{k_1 + \frac{\hat{K}_1(t)}{\ell}} \\ \frac{\rho^*_{d2}}{k_1 + \frac{\hat{K}_2(t)}{\ell}} \end{bmatrix} \end{aligned} \tag{38}$$

Therefore, when the saturation function (34) is used in the control law, the state error of the system cannot be convergent to zero but a special range which is dependent on the threshold value ℓ. The threshold value ℓ of the saturation function (34) should be chosen according to the inequality (38) once the permissible steady error of the system is given.

Design of DOB

In order to clearly describe the observer design, the regular system model with load disturbance for PMSM is given as

$$\begin{cases} \dot{x}_1(t) = A_{11}x_1(t) + A_{12}x_2(t) + dGT_l \\ \dot{x}_2(t) = A_{21}x_1(t) + A_{22}x_2(t) + u(t) + \rho(t) \end{cases} \tag{39}$$

where $d = 1/J_m$, $G = \begin{bmatrix} 0 \\ 1 \end{bmatrix}$.

A nonlinear observer[27] can be applied here to estimate the load disturbance T_l. The load DOB for PMSM is constructed as

$$\hat{T}_l = z + p(\omega_e) \tag{40}$$

$$\begin{aligned} \dot{z} = &- l(\omega_e)\frac{1}{J_m}z - l(\omega_e) \\ &\times \left(\frac{1}{J_m}p(\omega_e) - \frac{B_m}{J_m}\omega_e + \frac{1.5\varphi_m}{J_m}i_q\right) \end{aligned} \tag{41}$$

$$p(\omega_e) = h\omega_e \tag{42}$$

$$l(\omega_e) = \frac{\partial p(\omega_e)}{\partial \omega_e} = h \tag{43}$$

Associating with equation (39), neglecting the matched uncertainties which is already being controlled by improved NSMC and assumed that the deviation of load disturbance is bounded and $\lim_{t\to\infty} \frac{dT_l}{dt} = 0$,[22] the convergence of $\hat{T}_l$ is established as

$$\begin{aligned} \dot{\hat{T}}_l &= \dot{z} + \dot{p}(\omega_e) \\ &= -h\frac{1}{J_m}z - h\left(h\frac{1}{J_m}\omega_e - \frac{B_m}{J_m}\omega_e + \frac{1.5p\varphi_m}{J_m}i_q\right) + h\dot{\omega}_e \\ &= -h(\hat{T}_l - T_l) \end{aligned} \tag{44}$$

Therefore, the load disturbance estimation of $\hat{T}_l$ can track the load disturbance asymptotically in the limited time if h is chosen as $h > 0$.

Improved NSMC-DOB design for PMSM servo system

According to equation (4), the new nonlinear sliding surface for both matched uncertainties and mismatched uncertainties is given as

$$\begin{aligned} s(x,t) &= \begin{bmatrix} s_1(x,t) \\ s_2(x,t) \end{bmatrix} \\ &= \begin{bmatrix} F - \psi(y,r)A_{12}^T P & I_m \end{bmatrix} \begin{bmatrix} e_1(t) \\ e_2(t) \end{bmatrix} + \frac{1}{1.5p\varphi_m} G\hat{T}_l \end{aligned} \tag{45}$$

Supposed that the load disturbance error is defined as

$$e_T(t) = T_l - \hat{T}_l \tag{46}$$

which satisfies the following bounded condition

$$e_T^* = \sup_{t>0}(e_T(t)) \tag{47}$$

According to the observer asymptotically convergence performance described in equation (44), the bounded condition (47) for load disturbance estimation error is reasonable.

Theorem 1. The control law which is named as improved NSMC-DOB is given as follows

$$\begin{aligned} u(t) = & -\frac{d}{dt}\psi(y,r)A_{12}^T P e_1(t) + \sigma(t)\dot{x}_d(t) \\ & - \sigma(t)Ax(t) - \delta(t)G\hat{T}_l + k_1 s + \hat{K}(t) * sat(s) \end{aligned} \tag{48}$$

The controller (48) enforces the trajectory of (39) to move from any initial condition to the sliding surface in finite time and keep on it. In the above control law, the upper bounded of $\hat{K}(t)$ is chosen as follows

$$K_1^* > \Upsilon(1),\ K_2^* > \Upsilon(2) \tag{49}$$

where $\Upsilon = \left|\delta(t)G - \frac{Gh}{1.5p\varphi_m}\right| e_T^* + \begin{bmatrix} \rho_{d1}^* \\ \rho_{d2}^* \end{bmatrix}$.

Proof. Let a Lyapunov function for the system in equation (39) be defined as

$$V_3(t) = \frac{1}{2}s^T s \tag{50}$$

Taking the derivation of $V_3(t)$ and employing the control law (48) yields

$$\begin{aligned} \dot{V}_3(t) &= s^T \dot{s} \\ &= s^T \left(\begin{bmatrix} F - \psi(y,r)A_{12}^T P & I_m \end{bmatrix} \begin{bmatrix} \dot{e}_1(t) \\ \dot{e}_2(t) \end{bmatrix} + \begin{bmatrix} -\frac{d\psi(y,r)}{dt}A_{12}^T P & 0 \end{bmatrix} \begin{bmatrix} e_1(t) \\ e_2(t) \end{bmatrix} + \frac{1}{1.5p\varphi_m} G\dot{\hat{T}}_l \right) \\ &= s^T \left(\left(\delta(t)G - \frac{Gh}{1.5p\varphi_m} \right) e_T(t) - \rho(t) - k_1 s - \hat{K}(t) * sat(s) \right) \\ &< -k_1 s^T s + |s^T| \left(\left| \delta(t)G - \frac{Gh}{1.5p\varphi_m} \right| e_T^* + \begin{bmatrix} \rho_{d1}^* \\ \rho_{d2}^* \end{bmatrix} - \begin{bmatrix} K_1^* \\ K_2^* \end{bmatrix} \right) \end{aligned}$$

With the prerequisite condition of (49), the Lyapunov stability condition (50) has been satisfied as

$$\dot{V}_3(t) < 0$$

Therefore, under the condition of $k_1 > 0$, $h > 0$ and the improved NSMC-DOB control law (48), the sliding surface (45) based on DOB is asymptotically converging to a boundary layer set $\Omega = \{x | x \in \Re^4, |s_i(x,t)| \le \ell,\ i = 1,2\}$. When the width of the boundary layer ℓ is chosen appropriately according to equation (38), the permissible system state errors can be acquired inside the boundary layer.

Simulation results

In this section, the simulation is implemented in MATLAB/Simulink to verify the robust performance of PMSM servo system based on field-oriented control and the system block diagram is shown in Figure 2. It consists of the coordinate transformations of PMSM such as Clarke and Park transform, space vector pulse width modulation (SVPWM), DOB, and the control algorithm of improved NSMC-DOB.

The simulation is organized as follows. Firstly, the step trajectory tracking in PMSM servo system is used to verify the advantages of improved NSMC-DOB algorithm. The outstanding transient response performance of novel NSMC algorithm in equation (25) is highlighted by comparing with LSS controllers. The improved NSMC with the chattering reduction by saturation switching function and the adaptive parameter estimation is also illustrated. The insufficient in disposing the unmatched uncertainties of load disturbance in improved NSMC is described afterward. After that, the availability of DOB is verified by estimating the load disturbance. Finally, the improved NSMC-DOB is simulated for PMSM servo system to verify the proposed method effectively with the load disturbance rejection. Meanwhile, the sinusoidal and triangle trajectory tracking for PMSM servo system are simulated. This is used to highlight that the proposed improved NSMC-DOB algorithm can also decrease the tracking error for the continuous variable trajectory of PMSM mechanical angle.

The nominal parameters of PMSM are listed as follows

$$p = 2,\ \varphi_m = 0.175 \text{ V S}$$
$$R_s = 2.875\Omega,\ L_s = 0.0085H$$
$$B_m = 0.001 \text{ N m s},\ J_m = 0.0008 \text{ kg m}^2$$

In order to simulate the dynamical parameter perturbation in the process of PMSM running due to the motor temperature and magnetic field variation and verify the effectiveness of the proposed algorithm, the library file *powerlib.slx* in MATLAB/Simulink for PMSM is modified to add the disturbance to main

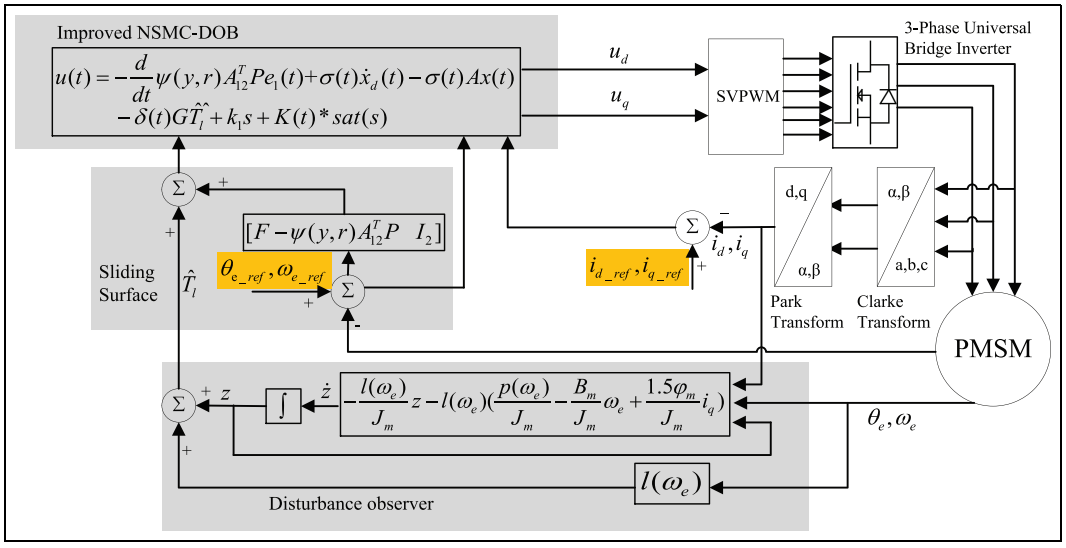

Figure 2. Structure of improved NSMC-DOB for PMSM servo system.

parameter R_s and L_s. A zero-mean-value random noise with Gaussian distribution is added to R_s and L_s in this article.

Step trajectory tracking simulation

In this section, the PMSM servo system is considered without load disturbance first to verify the performance of improved NSMC algorithm. According to the principle of NSMC, the fast response without overshoot of the control system is acquired by the variation of system damping ratio which is considered to change gradually from $\xi_1 = 0.5$ to $\xi_2 = 1$ in this article. The improved NSMC design parameters are as follows

$$\mu = 200,\ \beta = 3,\ \varepsilon = 0.001$$
$$\ell = 0.5,\ k_1 = 150$$
$$W = \begin{bmatrix} 3.86 \times 10^{-7} & 0 \\ 0 & 3.86 \times 10^{-7} \end{bmatrix}$$

According to the pole placement principle and the Lyapunov equation (17), the following parameter is acquired as

$$F = \begin{bmatrix} 0 & 0 \\ 0.1954 & 50.63 \end{bmatrix}$$
$$P = 10^{-7} \times \begin{bmatrix} 497.66 & -1.93 \\ -1.93 & 0.01497 \end{bmatrix}$$

For the comparison purpose to prove the performance of NSMC in PMSM servo system, the SMC with LSSs are designed based on the fixed damping ratio ξ and settling time t_s. Supposed that all the LSSs have the same dynamical resonance frequency ω_n and the following equation is used to choose the constant damping ratio and settling time

$$t_s = \frac{4}{\xi\omega_n} \tag{51}$$

The following LSSs are used in this article:

LSS-1 with $\xi = 0.5$ and $t_s = 0.195$ s;
LSS-2 with $\xi = 0.7$ and $t_s = 0.140$ s;
LSS-3 with $\xi = 0.9$ and $t_s = 0.110$ s.

The control law for LSS system can be acquired from (25) under the circumstances of $\psi(y,r) = 0$. The position reference is given as a step input $\theta_{r\_ref}(t) = 5$ (rad) with soft-start mode and the maximum speed limitation.

Figure 3 is the time response of the motor rotor angle with different sliding surfaces and the numerical

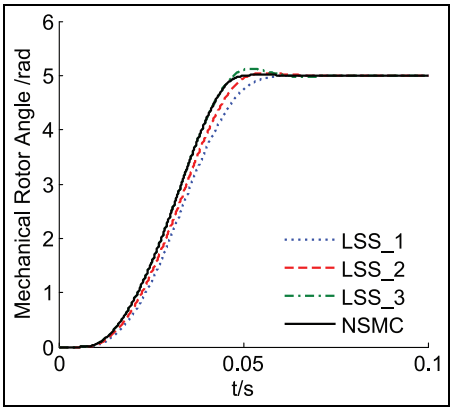

Figure 3. Time response of the motor rotor angle with different sliding surfaces.

Table 1. Performance parameter comparison of system response in different sliding surfaces.

Type of sliding surface	Overshoot (%)	Rising time (s)
LSS-1	2.5	0.0250
LSS-2	0.9	0.0264
LSS-3	0	0.0277
NSMC	0	0.0251

LSS: linear sliding surface; NSMC: nonlinear sliding mode control.

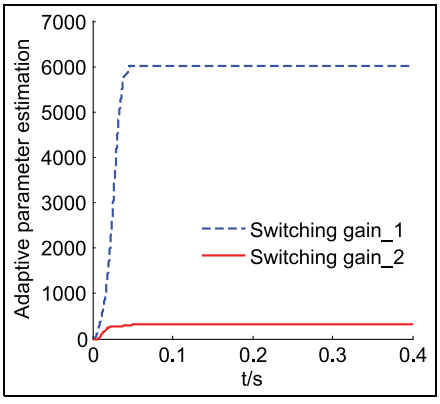

Figure 4. Adaptive parameter estimation for switching gains.

comparison for the system transient performance with overshoot and rising time is given in Table 1. The rising time is defined as the time required for the response to rise from 10% to 90% of final value. From Figure 3 and Table 1, it can be seen that the trajectory tracking of step position by NSMC can acquire the best performance with fast rising time and non-overshoot as well as high accuracy.

The adaptive parameter estimation used for two switching gains in improved NSMC control law is shown in Figure 4. Actually, the adaptive parameter estimation not only eliminates the necessity of the perturbation bound but also improves the system stability by estimating changeable uncertainties in the system. Figures 5 and 6 clearly show that the chattering in the control input and sliding surface is well suppressed by changing the switching function from sign function to saturation function.

In order to depict the effect of improved NSMC-DOB robustness to the mismatched uncertainties, the external load disturbance $T_l = 2.5\,\mathrm{N\,m}$ is exerted on the PMSM servo system at $t = 0.2\,\mathrm{s}$. Figure 7(a) shows the simulation results of the trajectory with step signal $\theta_{r\_ref}(t) = 5$ (rad), respectively, by improved NSMC and improved NSMC-DOB and the tracking error is illustrated in Figure 7(b). It can be clearly seen that the position error is reduced by the improved NSMC-DOB controller. For DOB equation (35), the parameter h is

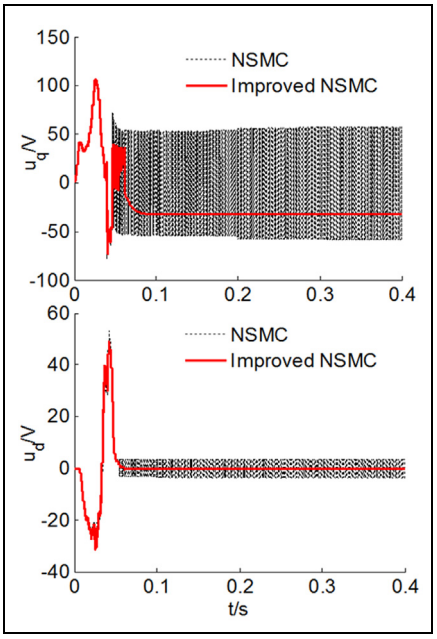

Figure 5. Control input of chattering reduction comparison between NSMC and improved NSMC.

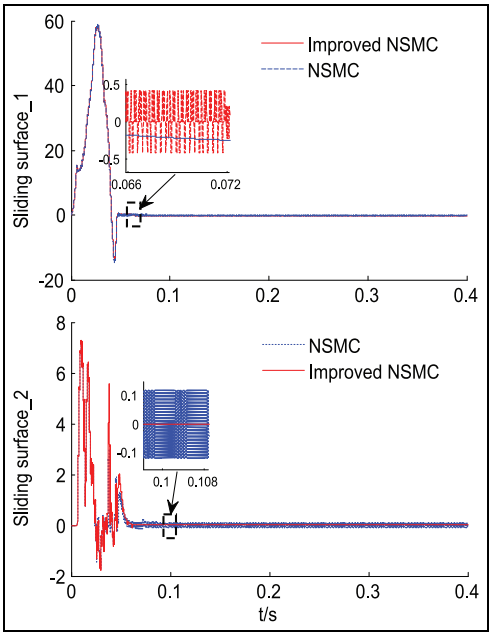

Figure 6. Sliding surfaces comparison between NSMC and improved NSMC.

chosen as $h = 1$. Figure 8 is the comparison of system state i_q, i_d and sliding surface of improved NSMC and improved NSMC-DOB in the presence of load disturbance. The sliding surface_2 is the current of i_d according to equation (45) which is shown in Figure 8(c).

From Figures 7 and 8, it can be seen that the improved NSMC fails to drive the motor position to

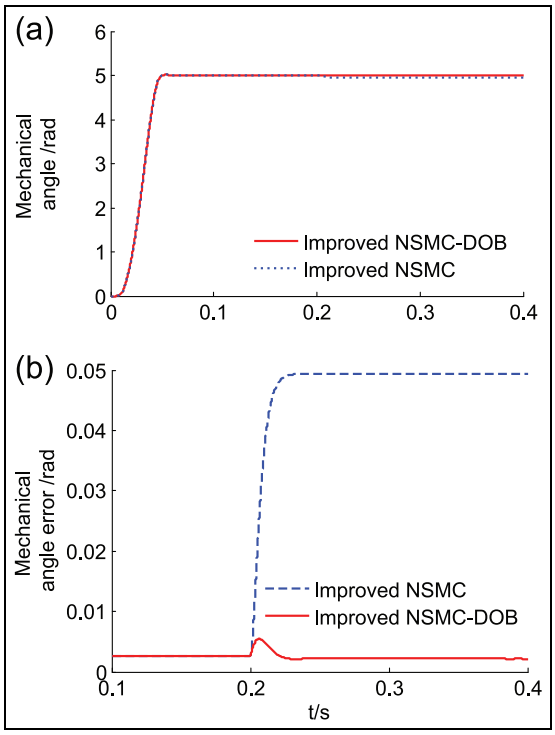

Figure 7. Comparison between improved NSMC and improved NSMC-DOB in the presence of load disturbance: (a) time response of motor rotor angle and (b) time response error of motor rotor angle.

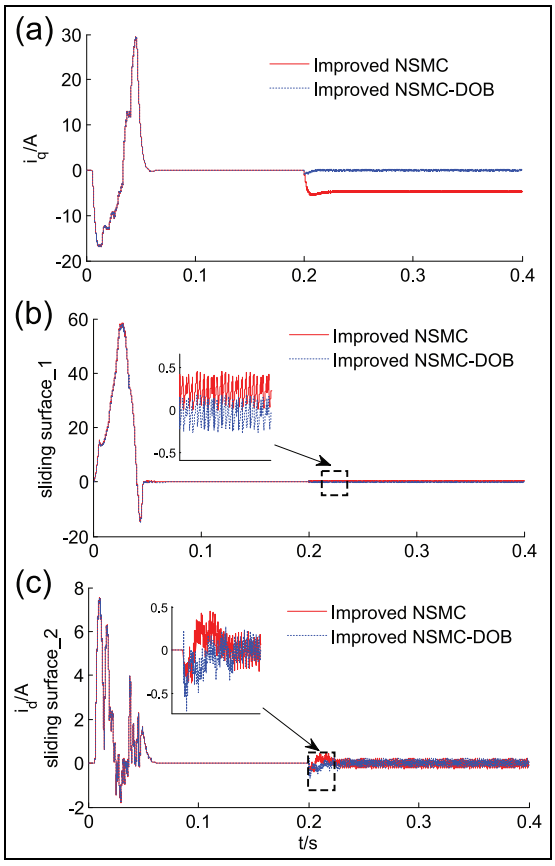

Figure 8. Comparison between improved NSMC and improved NSMC-DOB in the presence of load disturbance torque: (a) comparison of current i_q, (b) comparison of sliding surface_1 and (c) comparison of current i_d which is the sliding surface_2 as well.

the expected value in the presence of load disturbance while the proposed improved NSMC-DOB can suppress the mismatched load disturbance and have good tracking accuracy. The load disturbance is observed in Figure 9 and it can be seen that the DOB can estimate the load disturbance accurately.

Continuous variable trajectory tracking simulation

The sinusoidal and triangle trajectory is used in this section as the continuous variable trajectory. Figures 10(a) and 11(a), respectively, show the improved NSMC-DOB deducing the better response performance in dynamic PMSM trajectory tracking control for desired sinusoidal and triangle trajectory with the disturbance load torque $T_l = 2.5\,\mathrm{N\,m}$ exerted at $t = 0.6\,\mathrm{s}$ compared with improved NSMC control. From Figures 10(b) and 11(b), it can be clearly seen that the improved NSMC-DOB algorithm has a better trajectory tracking accuracy than improved NSMC after the load disturbance is exerted.

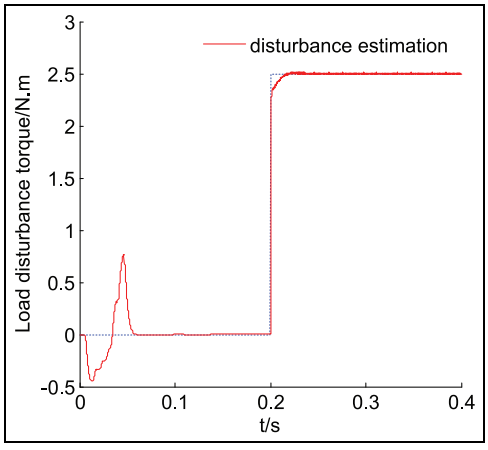

Figure 9. Load disturbance estimation.

Conclusion

In this article, an improved NSMC-DOB for PMSM servo system has been proposed. First, the nonlinear sliding surface is introduced in the SMC design. Then the adaptive parameter estimation has been designed for the switching gain to abolish the analysis necessity of the changeable uncertainties in the sliding switching

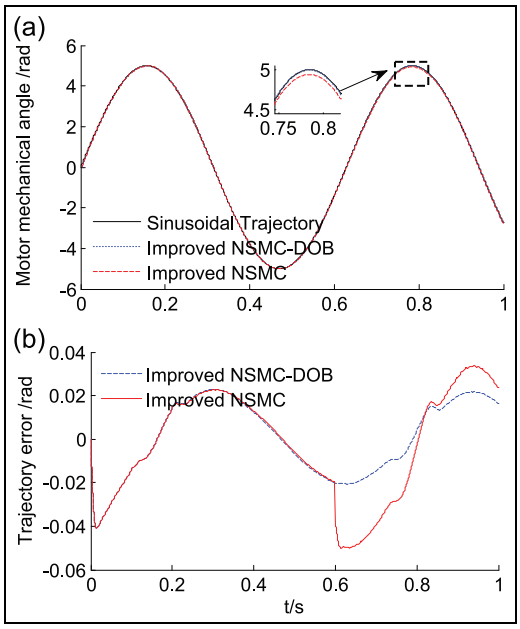

Figure 10. Dynamic response for sinusoidal trajectory: (a) time response of motor angle and (b) time response error of motor angle.

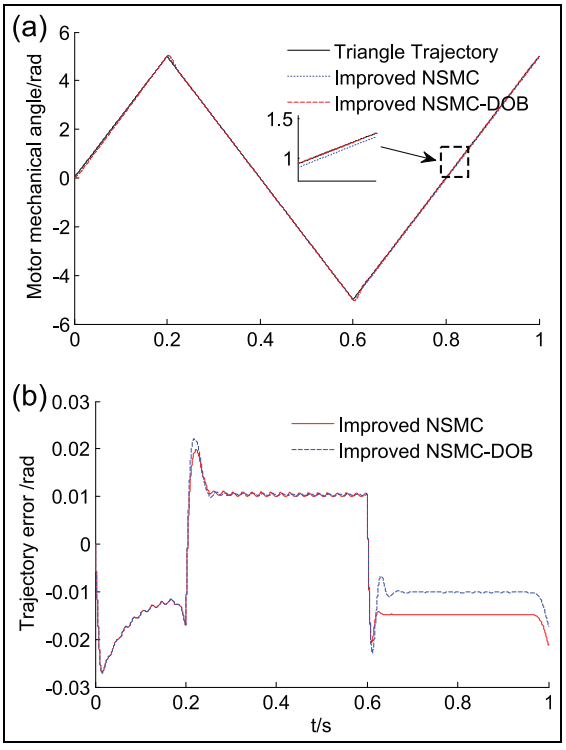

Figure 11. Dynamic response for triangle trajectory: (a) time response of motor angle and (b) time response error of motor angle.

part. Meanwhile, the sign switching term is replaced with a saturation function to acquire a low chattering performance under the permissible system errors. A DOB has been designed and combined with improved NSMC to solve the problem of its unrobustness to the mismatched disturbance. The simulation results shows that the proposed improved NSMC-DOB applied in PMSM servo system not only acquires the better transient response but also realizes the robustness to the system parameter uncertainties and perturbations including the matched and mismatched disturbance. The robustness to system mismatched disturbance can increase the positioning accuracy to some extent which is beneficial to amount of servo systems.

Declaration of conflicting interests

The author(s) declared no potential conflicts of interest with respect to the research, authorship, and/or publication of this article.

Funding

The author(s) disclosed receipt of the following financial support for the research, authorship, and/or publication of this article: This paper is funded by the CASHIPS Director's Funds (Grant No. YZJJ201521) and Changzhou Sci & Tech Program (Grant No. CE20140025).

References

1. Krishman R. *Electric motor drives: modeling, analysis, and control*. Upper Saddle River, NJ: Prentice Hall, 2001.
2. Liu H and Li S. Speed control for PMSM servo system using predictive functional control and extended state observer. *IEEE T Ind Electron* 2012; 59: 1171–1183.
3. Huang J, Li H, Chen Y, et al. Robust position control of PMSM using fractional-order sliding mode controller. *Abstr Appl Anal* 2012; 2012: 1–33.
4. Zhang X, Sun L, Zhao K, et al. Nonlinear speed control for PMSM system using sliding-mode control and disturbance compensation techniques. *IEEE T Power Electr* 2013; 28: 1358–1365.
5. Sree Lakshmi G, Kamakshaiah S and Das TR. Closed loop PI control of PMSM for hybrid electric vehicle using three level diode clamped inverter for optimal efficiency. In: *International conference on energy efficient technologies for sustainability*, Nagercoil, India, 10–12 April 2013, pp.754–759. New York: IEEE.
6. Mehta H, Joshi V, Thakar U, et al. Speed control of PMSM with hall sensors using DSP TMS320f2812. In: *IEEE 11th international conference on power electronics and drive systems*, Sydney, NSW, Australia, 9–12 June 2015, pp.295–300. New York: IEEE.
7. Qi L and Shi H. Adaptive position tracking control of permanent magnet synchronous motor based on RBF fast terminal sliding mode control. *Neurocomputing* 2013; 115: 23–30.
8. Liu X, Wu Y and Liu B. The research of adaptive sliding mode controller for motor servo system using fuzzy upper bound on disturbance. *Int J Control Autom* 2012; 10: 1064–1069.

9. Errouissi R, Ouhrouche M, Chen W, et al. Robust nonlinear predictive controller for permanent-magnet synchronous motors with an optimized cos function. *IEEE T Ind Electron* 2012; 59: 2849–2858.
10. Maier S, Bals J and Bodson M. Periodic disturbance rejection of a PMSM with adaptive control algorithms. In: *IEEE international electric machines & drives conference (IEMDC)*, Niagara Falls, ON, Canada, 15–18 May 2011, pp.1070–1075. New York: IEEE.
11. Ramírez GVG, Valdés LGV, Medina MA, et al. Adaptive nonlinear control of induction motor. *Int J Control Autom* 2011; 9: 176–186.
12. Choi HH, Vu NTT and Jung J-W. Digital Implementation of an adaptive speed regulator for a PMSM. *IEEE T Power Electr* 2011; 26: 3–8.
13. Çelík E and Öztürk N. An adaptive PI controller schema based on fuzzy logic controller for speed control of permanent magnet synchronous motors. In: *4th international conference on power engineering, energy and electrical drives*, Istanbul, 13–17 May 2013, pp.715–720. New York: IEEE.
14. Ghafari-Kashani AR, Faiz J and Yazdanpanah MJ. Integration of non-linear H_∞ and sliding mode control techniques for motion control of a permanent magnet synchronous motor. *IET Electr Power App* 2010; 4: 267–280.
15. Zhang DQ and Panda SK. Chattering-free and fast-response sliding mode controller. *IEE P: Contr Theor App* 1999; 146: 171–177.
16. Li S, Zhou M and Xinghuo Y. Design and implementation of terminal sliding mode control method for PMSM speed regulation system. *IEEE T Ind Inform* 2013; 9: 1879–1891.
17. El-Sousy FFM. Robust wavelet-neural-network sliding-mode control system for permanent magnet synchronous motor drive. *IET Electr Power App* 2011; 5: 113–132.
18. Leu VQ, Choi H and Jung J-W. Fuzzy sliding mode speed controller for PM synchronous motors with a load torque observer. *IEEE T Power Electr* 2012; 27: 1530–1539.
19. Zhao F, Liu Y, Yao X, et al. Integral sliding mode control of time-delay systems with mismatching uncertainties. *J Syst Eng Electron* 2010; 21: 273–280.
20. Leu VQ, Choi HH and Jung J-W. LMI-based sliding mode speed tracking control design for surface-mounted permanent magnet synchronous motors. *J Electr Eng* 2012; 7: 513–523.
21. Zhang J, Shi P and Xia Y. Robust adaptive sliding-mode control for fuzzy systems with mismatched uncertainties. *IEEE T Fuzzy Syst* 2010; 18: 700–711.
22. Yang J, Li S and Xinghuo Y. Sliding-mode control for systems with mismatched uncertainties via a disturbance observer. *IEEE T Ind Electron* 2013; 60: 160–169.
23. Ginoya D, Shendge PD and Phadke SB. Sliding mode control for mismatched uncertain systems using an extended disturbance observer. *IEEE T Ind Electron* 2014; 61: 1983–1992.
24. Lin Z, Pachter M and Banda S. Toward improvement of tracking performance nonlinear feedback for linear system. *Int J Control* 1998; 70: 1–11.
25. Bandyopadhyay B, Fulwani D and Fridman L. *Sliding mode control using novel sliding surface*. London: Springer, 2010.
26. Plestan F, Shtessel Y, Brégeault V, et al. New methodologies for adaptive sliding mode control. *Int J Control* 2010; 83: 1907–1919.
27. Chen W. Nonlinear disturbance observer- enhanced dynamic inversion control of missiles. *J Guid Control Dynam* 2003; 26: 161–166.

Appendix 1

Notation

B_m	equivalent viscous friction coefficient of motor
i_d, i_q	d and q axis stator current
J_m	equivalent moment of inertia of motor
p	numbers of pole pairs
R_s, L_s	stator resistance and inductance
T_e, T_l	motor electromagnetic torque and load disturbance
u_d, u_q	d and q axis stator voltage
θ_r, θ_e	motor rotor mechanical and electrical angle
φ_m	permanent magnet flux linkage
ω_r, ω_e	motor rotor mechanical and electrical angular velocity